Fusion Engineering and Design 192 (2023) 113616

Contents lists available at ScienceDirect

Fusion Engineering and Design

journal homepage: www.elsevier.com/locate/fusengdes

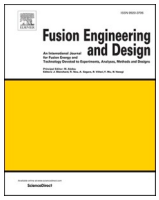

Control strategy for the magnetic energy storage and transfer system (MEST)

Francesco Lunardon [a,*], Alberto Maistrello [b], Elena Gaio [b], Roberto Piovan [b]

[a] Università degli Studi di Padova, Italy
[b] Consorzio RFX, Corso Stati Uniti 4, Padova I-35127, Italy

ARTICLE INFO

Keywords:
Power supply system
Superconducting magnetic energy storage system

ABSTRACT

The Magnetic Energy Storage and Transfer system (MEST) aims at improving the power handling in supplying the SuperConducting (SC) coils of fusion experiments. It is based on smart use of Superconducting Magnetic Energy Storage technology and allows the introduction of a certain degree of decoupling between the grid and the load. The MEST operation is based on the storage and transfer of the needed energy between the Load Coil (LC) and an additional storage inductor named Sink Coil (KC); the energy transfer is realized via capacitors switched by fully controllable semiconductors.

This paper focuses on the control system of the MEST and proposes a control strategy, based on two decoupled control loops, with the aim both to guarantee the desired current on the load coil and the compensation of the system losses. A model of the MEST with the proposed control system has been developed to analyze the performance through numerical simulations. The control strategy and the simulation results will be presented and discussed in the paper.

1. Introduction

The Magnetic Energy Storage and Transfer system (MEST) is an alternative solution to the thyristor-based converters which supply the main SuperConducting (SC) coils of most existing fusion experiments. It can give a partial or a complete degree of decoupling between the grid and the magnets, which means that the power demand to supply the coils is not instantly supplied by the network [1]. The MEST would substitute thyristor-based converters and would be used as Energy Storage System, demanding to the grid only the power to compensate for the losses and to sustain the plasma against resistive dissipation, with a slower dynamic than the one required by the SC coils.

As we get closer to the development of a demonstration fusion reactor for electrical energy production, electrical power management is becoming a crucial aspect in the Coil Power Supply (CPS) system design and in general, in the plant electrical system design.

This improvement of the power handling will be crucial in future large fusion experiments because active power peaks required during the gas breakdown, plasma current ramp-up and plasma disturbances control, increase with the size of the machine and the plasma current value [2].

In ITER, the active power peak is expected to reach up to 600 MW, while the reactive power will overcome 900 MVar [3] during almost all the plasma pulse. In the EU DEMO, the studies conducted so far [4] give higher estimated values, especially for the reactive power. The foreseen peaks of active power in large fusion reactors like EU DEMO slightly overcome the limitations usually imposed by the grid operators, both in terms of absolute value and variation in time. Under these assumptions, the use of electric energy storage systems in medium-size and large fusion reactors is expected to become mandatory to reduce the active power demand and smooth its profile. On the other hand, the reactive power exchanged between the SC coils power supplies and the grid has to be limited and controlled by using advanced converter technologies. In fact, the use of thyristor-based converters only, robust and cost-effective technology largely used in all fusion experiments, also in ITER, seems not suitable for supplying SC coils when scaled to large-size experiments due to the too huge reactive power demand [4].

The MEST circuit already studied in [5] and [1] is shown in Fig. 1. The system operates by transferring energy between the Load Coil (LC), the superconducting coil to be supplied, and the Sink Coil (KC), an additional superconducting coil that acts as an energy reservoir. The energy transfer system can control the LC voltage only if KC current (i_{KC})

* Corresponding author.
E-mail address: francesco.lunardon@igi.cnr.it (F. Lunardon).

https://doi.org/10.1016/j.fusengdes.2023.113616
Received 31 October 2022; Received in revised form 3 February 2023; Accepted 28 February 2023
Available online 16 March 2023

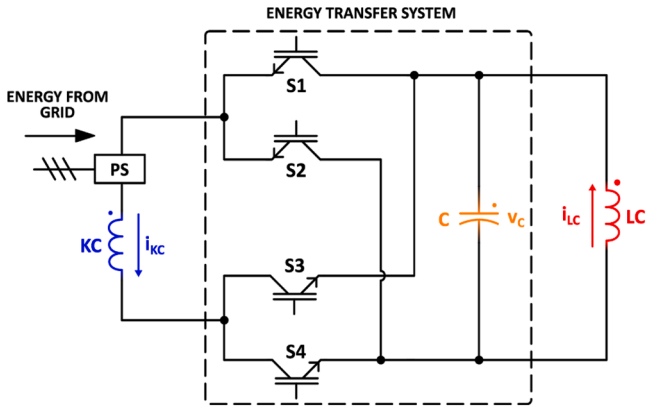

Fig. 1. MEST principle scheme.

is greater than the absolute value of LC current ($|i_{LC}|$), this condition will be explained and justified in Section 2.1. To comply with this condition a Power Supply (PS) has to feed the initial energy to the KC, to compensate the circuit losses and to provide the power to be transferred to the plasma, magnetically coupled to LC, for its ignition, sustainment and control. The energy transfer system of the MEST is composed of four equivalent switches (S1, S2, S3 and S4), each comprising fully controllable semiconductor switches (like IGCTs or IGBTs) with all the appropriate devices for their operation (series connected diodes if the component is asymmetric, snubbers and clamp circuits) and a capacitor bank (C).

The energy transfer between the two SC coils is performed by controlling the voltage of C (v_C), thus the voltage across LC, applying a proper switching pattern of the four equivalent switches (S1÷S4), following a hysteresis logic, as explained in Section 2.1.1) and Section 2.1.2). The use of a switched capacitor for the energy transfer allows for reaching a unitary efficiency, except for the circuit losses. The capacitor bank (C) is not meant to store energy but only to achieve the energy transfer between KC and LC, thus it is designed to be as small as possible compatibly with the switching frequency. Its capacitance value, along with the amplitude of the hysteresis, is inversely proportional to the switching frequency; in particular, the reduction of C capacitance implies a higher switching frequency of the four switches, for a given switching pattern, and this implies higher commutation losses and therefore a higher number of components to be used for each equivalent switch.

The two main variables to be controlled in the MEST system are LC current (i_{LC}) and KC current (i_{KC}). To isolate the controlled variables from influences that would otherwise disturb them two isolated control loops are required. Such a design is referred to as decoupling control.

In Sections 2.1 and 2.2 the control strategy to control i_{LC} and i_{KC} with two decoupled control loops is proposed.

2. MEST control system

With the control system proposed in this section, the PS is devoted to controlling i_{KC} while the energy transfer system (consisting of C and S1…S4) controls i_{LC} through the modulation of v_C. In this way, the decoupling between i_{LC} control and i_{KC} control is achieved. In Fig. 2 the block diagram of the MEST control system is reported.

2.1. Load coil current (i_{LC}) control strategy

The variable to be controlled is the load current (i_{LC}), thus the main reference signal is the desired load current ($i_{LC,ref}$). The LC current control is performed by two different blocks: the "LC current control" and "Voltage hysteresis control" blocks of Fig. 2.

The "LC current control" is a Proportional Integral (PI) controller that takes as input the measurement of i_{LC} and the reference $i_{LC,ref}$ generating a reference waveform for the load voltage ($v_{C,ref}$).

The "Voltage hysteresis control" takes as input $v_{C,ref}$ and changes the topology of the MEST circuit acting on the command of the four equivalent switches (closed or open) in order to maintain the MEST output voltage (v_C) within a hysteresis band.

The different circuit topologies, called states and described in 1),

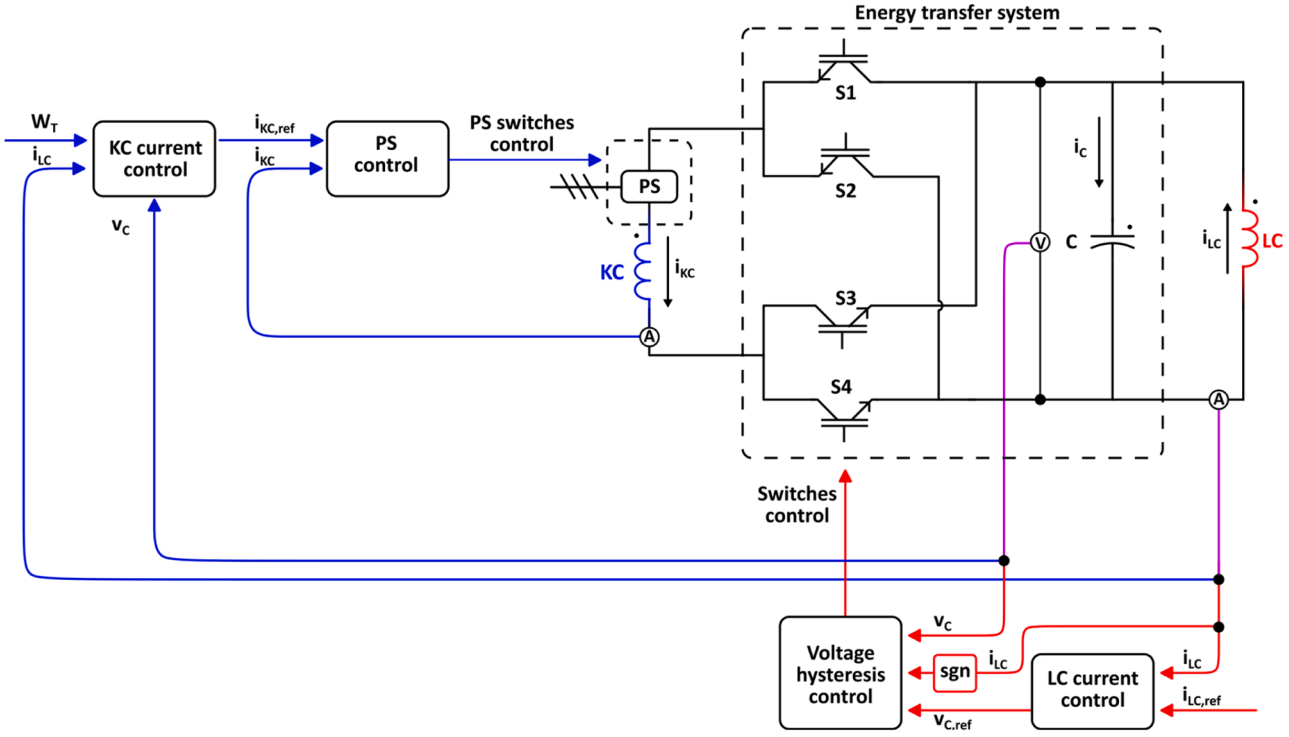

Fig. 2. Block diagram of the MEST control system.

Table 1
Relevant states of the MEST system and trends of main variables neglecting circuit losses with $i_{LC}>0$.

State	dv_C/dt ($i_{LC}>0$)	dv_C/dt ($i_{LC}<0$)	i_C
A=[1 0 0 1]	<0	<0 w/high derivative	i_{KC}-i_{LC}
B=[0 1 0 1]	>0	<0	i_{LC}
C=[1 0 1 0]	>0	<0	i_{LC}
D=[0 1 1 0]	>0 w/ high derivative	>0	i_{KC}+i_{LC}

follow each other in patterns generated by the hysteresis control as described in 2). During the system operation, the two nested loops continue operating to assure the desired current waveform in the load. In Fig. 2 the double control loop of i_{LC} is highlighted in red.

2.1.1. Switching states

In Table 1 the relevant states of the MEST are reported, where 1 indicates a closed switch and 0 is an open switch, with the time derivatives of the circuit variables.

A detailed explanation of all the MEST states can be found in [1] and in this section, only the states for $i_{LC}>0$ will be recalled in detail.

From Table 1 it can be noticed that with $i_{LC} > 0$ there are three states to increase v_C and one to decrease v_C, while with $i_{LC} < 0$ there are three states to decrease v_C and one to increase v_C.

The most important constraint of the control is that i_{KC} must be always greater than $|i_{LC}|$ otherwise the behavior of the circuit expected by the control system do not occur. If this condition is not satisfied, v_C cannot be decreased when i_{LC} is positive and v_C cannot be increased when i_{LC} is negative.

The hysteresis control band is defined by the Lower Limit (LL) and the Upper Limit (UL), which are set above and below the reference voltage $v_{C,ref}$.

- State *B*=[0,1,0,1] or C=[1,0,1,0] with $i_{LC}>0$

These two states are equivalent and when they are applied KC is short-circuited by S1 and S3 or by S2 and S4. In this way, i_{KC} remains constant and also the KC energy. Considering $i_{LC}>0$, v_C increases from LL to UL of the hysteresis band. If v_C is greater than 0 part of LC energy is transferred to C (Fig. 3a) and if v_C is lower than zero part of the energy stored in C is transferred to KC (Fig. 3b).

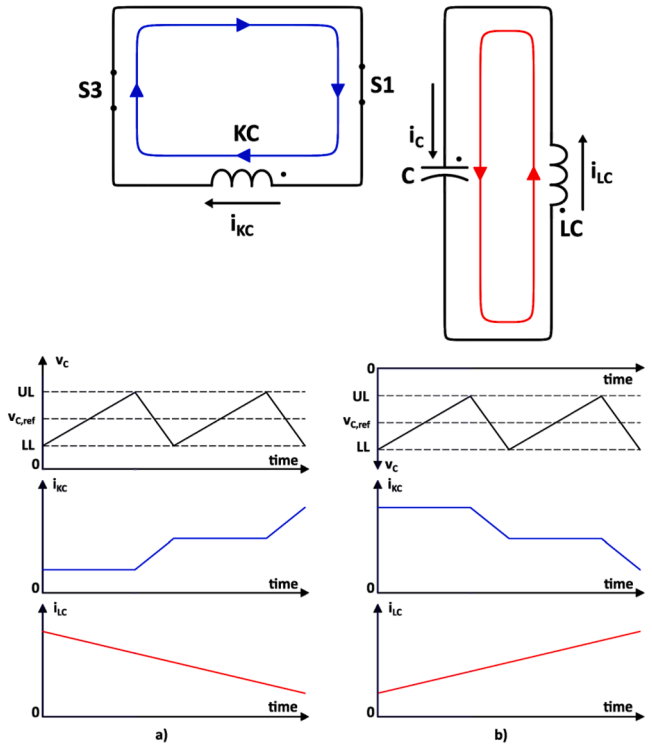

Fig. 3. State C=[1,0,1,0] and v_C, i_{KC} and i_{LC} trends.

- State *A*=[1,0,0,1]

State A is the only state that can be used to decrease v_C when $i_{LC} >0$, this is the reason why i_{KC} shall be always greater than $|i_{LC}|$. If $|i_{LC}| > i_{KC}$ and $i_{LC} > 0$ imposing the state *A*=[1001], for Kirchhoff's current law, $i_C > 0$ so v_C increases instead of decreasing and an undamped oscillation between KC, LC and C is observed. In this state, since $i_{KC}>|i_{LC}|$, the capacitor voltage decreases from UL to LL. If v_C is positive, part of LC and C energy is transferred to KC (Fig. 4a). If v_C is negative part of KC energy is transferred both to LC and C (Fig. 4b).

- State *D*=[0,1,1,0]

With this state the current entering the capacitor is $i_C=i_{KC}+i_{LC}$ then the capacitor voltage increases from LL to UL. If v_C is positive both i_{KC} and i_{LC} decrease and part of KC and LC energy is transferred to C (Fig. 5a). If v_C is negative both i_{KC} and i_{LC} increase and part of C energy is transferred to KC and LC (Fig. 5b). This state is called "high derivative state" because it leads to the maximum derivative for the load voltage (i.e. C and LC voltage) and can be used when a fast variation of the load voltage is required, as explained in Section 3. If $|i_{LC}| > i_{KC}$ and $i_{LC} < 0$ imposing the state *D*=[0110], for Kirchhoff's current law, $i_C < 0$ so v_C decreases instead of increasing and an undamped oscillation between KC, LC and C is observed.

2.1.2. Switching patterns

The control system can operate with different patterns of the states to maintain v_C within the hysteresis band limits (LL and UL).

At the beginning of the MEST development, a single-leg switching pattern was adopted. This switching pattern focuses the commutations on S1 – S2 to modulate v_C and S3 – S4 commutate only when i_{LC} changes polarity. The states sequence A,B,A,B… is adopted when $i_{LC}>0$ and D,C, D,C… when $i_{LC}<0$. With the single-leg switching pattern the commutations are in charge of S1 and S2 while S3 and S4 alternately carry i_{KC} depending on i_{LC} polarity.

The switching pattern proposed in this paper, called the double-leg switching pattern, focuses on the equalization of the commutation between the four equivalent switches:

- With $i_{LC}>0$ the sequence of the states for controlling v_C is A-B-A-C-A-B-A-C…
- With $i_{LC}<0$ the sequence of the states for controlling v_C is D-B-D-C-D-B-D-C…

The adopted states sequences lead to equalizing the switching losses between all four switches. This implies that the switching frequency of S1 and S2 is halved, in comparison with the single-leg switching pattern, for a given capacitance of C. In other terms, with the double-leg control strategy, the C capacitance could be halved for a given limit on the switching frequency. This can be seen in the simulation results in Section 3.

1) *Patterns with increased dynamic performance*

States D (with $i_{LC}>0$) and A (with $i_{LC}<0$) lead always to a higher derivative of v_C when compared to the other states. This behavior derives from the fact that the capacitor current module $|i_C|$ during these states is equal to $i_{KC}+|i_{LC}|$ (see Table 1) and is always higher than $|i_C|$ in the other states, which are equal to $i_{KC}-|i_{LC}|$ or i_{LC}. Fig. 6 reports the different i_C values, depending on the states, when varying i_{LC} from its minimum to its maximum value ($i_{LC,max}$ is the maximum LC current

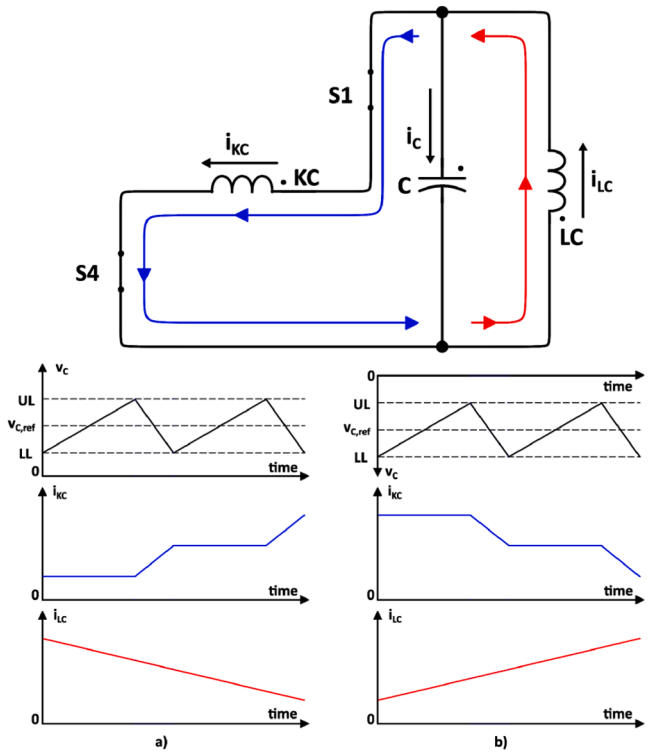

Fig. 4. State A=[1,0,0,1] and v_C, i_{KC} and i_{LC} trends.

during the scenario and $i_{KC,min}$ is the minimum KC current during the scenario).

It has to be noted that the use of patterns that comprise high voltage derivative states leads to the commutation of all four switches at each change of state (for instance if a sequence A-D-A-D… is imposed). Therefore the two high voltage derivative states should be avoided during operation when the reference $v_{C,ref}$ is close to v_C, so when the dynamic of the system is sufficient, to keep the switching frequency within the design limit of the single equivalent switches. The high voltage derivative states are used to increase the dynamic performance when $|v_{C,ref} - v_C| > \Delta V_{C,thr}$, with $\Delta V_{C,thr}$ a defined value, to increase (with $i_{LC}>0$) or decrease (with $i_{LC}<0$) v_C with the highest dynamic, and to follow as fast as possible $v_{C,ref}$.

In Section 3 simulation results with the use of the high voltage derivative states are reported.

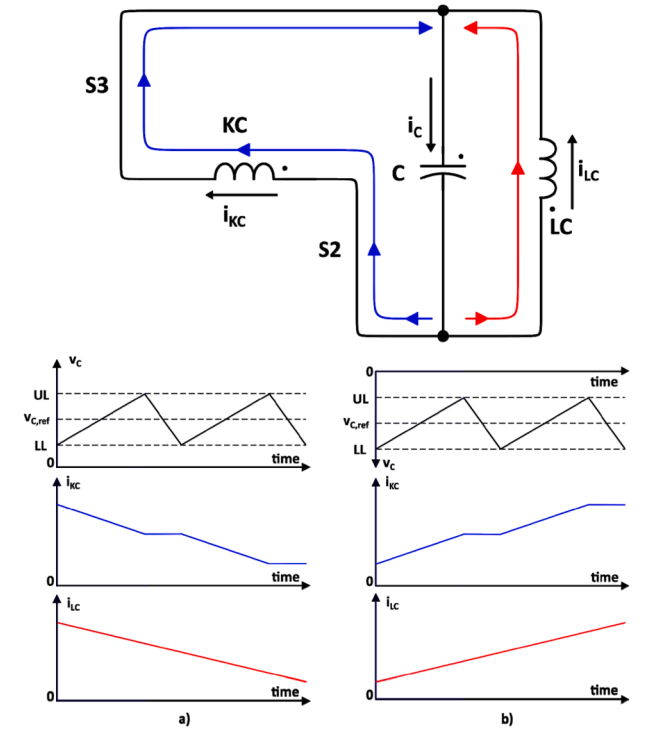

Fig. 5. State D=[0,1,1,0] and v_C, i_{KC} and i_{LC} trends.

2.2. Sink coil current (i_{KC}) control strategy

During system operation, the PS has to compensate for the circuit losses and supply the power to the plasma. In other words, PS has to maintain constant the energy of the system during the pulse and this is achieved by the control of i_{KC}. The i_{KC} control double loop (highlighted in blue in Fig. 2) involves "KC current control" and "PS control" blocks. The first has as inputs the v_C, i_{LC} and the total energy of the system W_T. KC has to store before the pulse at least double of the maximum energy stored by LC during the foreseen scenario. On the basis of the maximum current value desired in the load coil during the pulse scenario ($I_{LC,max}$), the total energy in the circuit can be calculated:

$$W_T = \frac{1}{2}L_{KC}I_{LC,max}^2 + \frac{1}{2}L_{LC}I_{LC,max}^2 = W_{KC,min} + W_{LC,max} \quad (1)$$

Where L_{KC} and L_{LC} are KC and LC inductances respectively. Then the block gives as output the KC current reference ($i_{KC,ref}$) to maintain constant the system energy. $i_{KC,ref}$ is derived as follows:

$$i_{KC,ref}(t) = \sqrt{\frac{2(W_T - w_{LC}(t) - w_C(t))}{L_{KC}}} \quad (2)$$

Considering the energy stored in the capacitor bank C equal to (C is the capacitance of the capacitor bank):

$$w_C(t) = \frac{1}{2}Cv_C^2(t) \quad (3)$$

The "PS control" block is a PI controller that takes as input the measurement of i_{KC} and the reference $i_{KC,ref}$ and controls the PS to maintain near zero the difference between the two input signals. With this control scheme, the energy of the system remains constant during the pulse as can be seen in Section 3.

3. Numerical model and simulation results

A detailed numerical model of the MEST circuit and control system has been developed in Simulink to evaluate the control strategy performance supplying a single SC coil. The MEST operation has been simulated with values of voltage, current and LC inductance compatible with the power supply of a main poloidal field coil of a large tokamak

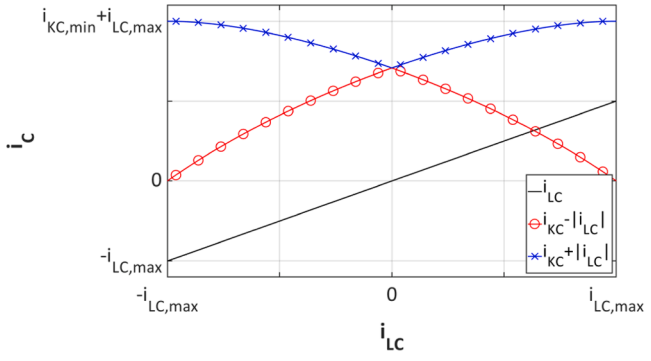

Fig. 6. i_C trends when varying i_{LC} from its minimum to its maximum value considering L_{LC}=L_{KC}.

Table 2
Parameters used in the numerical simulations.

Parameter	Value
LC inductance	2 H
KC inductance	2 H
C capacitance	7 mF
Rated voltage	8 kV
Hysteresis band	±800 V (10% of the rated voltage)

reactor, comparable to ITER or EU DEMO. The numerical model neglects the magnetic coupling between the poloidal field coils of the reactor and between LC and the plasma. The capacitance C value has been chosen to maintain the maximum switching frequency of the switches under 500 Hz considering the double-leg switching pattern. This limit has been chosen as a tradeoff between dynamic performance and switching losses considering the power level of a medium-large sized tokamak. The simulations are performed using the two different switching patterns with the same value of the C capacitance to allow the comparison between the two patterns.

In Table 2 parameters used in the simulations can be found.

The MEST operation supplying one of the main poloidal field coils during a plasma pulse comprises 5 phases, three of them cyclically repeated:

- KC pre-charge: KC is pre-charged by the PS.
- Phase 1: part of the energy stored in KC is transferred to LC thus LC current is pre-charged to its initial value to begin the pulse.
- Phase 2: during the plasma pulse (divided in breakdown, ramp-up, flat-top and ramp-down of the plasma current) the energy is transferred between KC and LC.
- Phase 3: at the end of the plasma pulse the energy in LC is transferred to KC. Then phase 1 can take place or, if a reactor shutdown is foreseen, KC is discharged (not shown in Fig. 7).
- KC discharge: the PS transfer the KC energy into the grid.

A more detailed explanation of the different phases can be found in [1].

Fig. 7 shows i_{LC}, i_{KC} and v_C during the simulation of the MEST supplying LC following the typical trend of the current applied to a sector of the central solenoid during a tokamak pulse.

The same simulation scenario has been carried out with the single-leg strategy and the double-leg strategy. In Figs. 8 and 9 it can be seen that the frequency during the simulation with the double-leg strategy leads to a decrease of the maximum switching frequency from 680 Hz to below 340 Hz. In Fig. 8 it can be seen that with the single-leg switching pattern only S1 and S2 commutates with the same frequency, to control

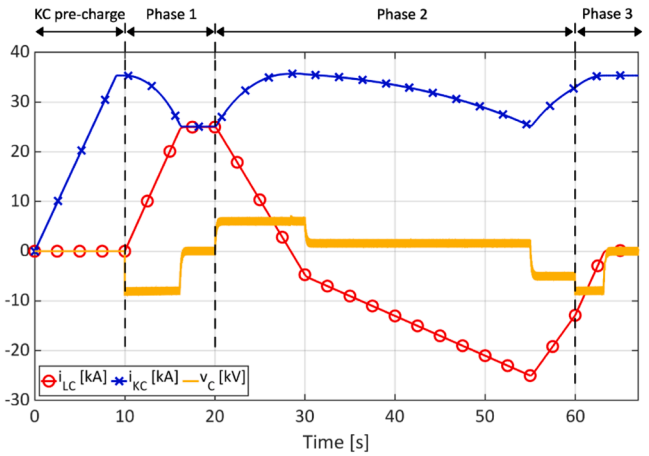

Fig. 7. Waveforms of the main MEST variables during the plasma pulse.

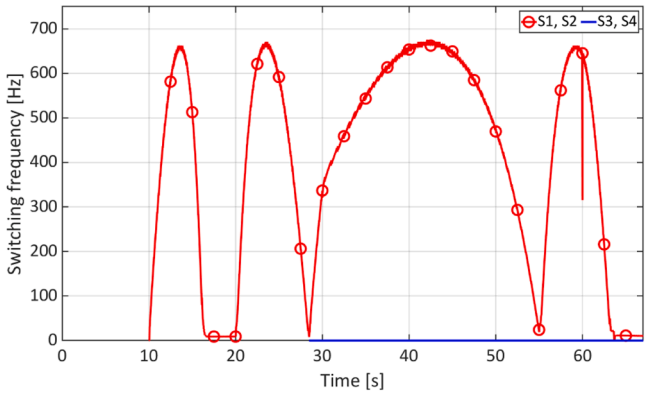

Fig. 8. Switching frequency of S1÷S4 during the pulse simulation with single-leg switching pattern.

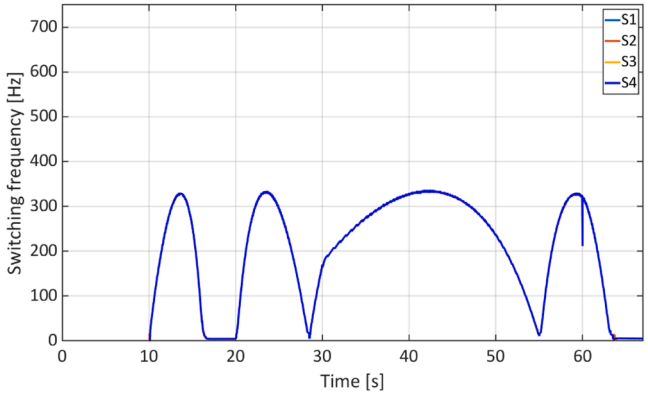

Fig. 9. Switching frequency of S1÷S4 during the pulse simulation with double-leg switching pattern.

the load voltage, while S3 and S4 commutates only when i_{LC} changes polarity, therefore their switching frequency is zero. In Fig. 9 the switching frequencies of the four switches are the same during the whole pulse and therefore results overlapped. These results can be explained by the fact that the commutations are distributed between all four switches. In this way, the maximum switching frequency can be halved using the same C capacitance value or the C capacitance can be halved for a given value of maximum switching frequency.

Fig. 10 shows the results of numerical simulations in which $v_{C,ref}$ has a step variation from −8 kV to +8 kV (i_{LC}≈27 kA and i_{KC}≈37 kA in the moment of $v_{C,ref}$ variation, C = 7.2 mF). The red line reports v_C variation without the use of the high derivative state and it rises to the new $v_{C,ref}$ value in about 4 ms while the blue line reports v_C variation with the high derivative state $D = [0,1,1,0]$ and v_C reaches the new references in about 2 ms.

The results show that the dynamic response of the MEST following the load voltage (v_C) can be significantly increased with the use of the high derivative states. As it can be seen in Fig. 6, the dynamic performance increase is maximum when $i_{LC}=\pm i_{LC,max}$ and it is negligible when i_{LC} is close to 0 A.

In Fig. 11 the energies of KC, LC, C and their sum are shown during the pulse of Fig. 7. After the initial KC pre-charge the energy is maintained at a constant value by the i_{KC} control that acts on the PS. As expected by the system and control design the C energy is negligible with respect LC and KC ones, and in this simulation, the max C energy is four orders of magnitude lower than the total one.

4. Conclusions

The MEST system is composed of two main sections: the energy

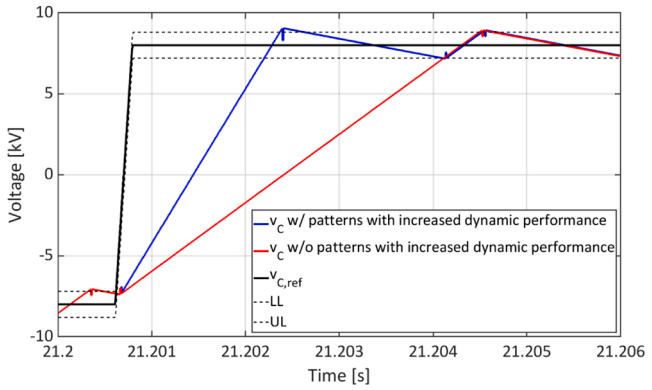

Fig. 10. v_C variation from −8 kV to 8 kV with and without the use of patterns with increased dynamic performance (i_{LC}≈27 kA, i_{KC}≈37 kA in the moment of $v_{C,ref}$ variation, C = 7.2 mF).

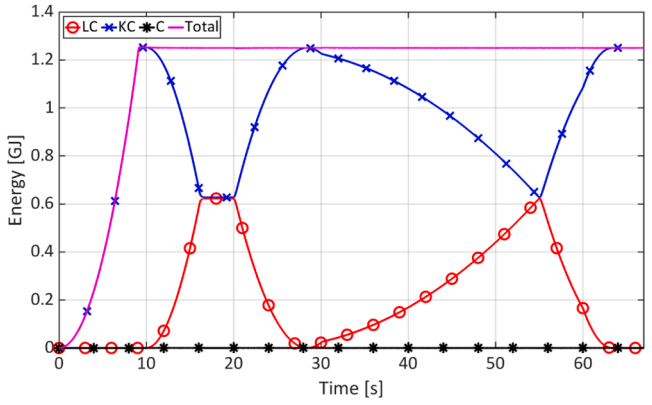

Fig. 11. LC, KC, C and total energy during the MEST pulse.

transfer system that transfers the energy between the two SC coils applying patterns of states and a second one that controls the PS to compensate for the circuit and plasma losses. The proposed switching patterns lead to an optimization of the capacitor bank design and also increase the dynamic performance of the system. In the paper, the circuit and plasma losses compensation method is presented and operated in the control to maintain constant the energy of the system. The numerical simulations confirm the effectiveness of the control strategy proposed.

Declaration of Competing Interest

The authors declare that they have no known competing financial interests or personal relationships that could have appeared to influence the work reported in this paper.

Data availability

No data was used for the research described in the article.

Acknowledgments

This work has been carried out within the framework of the EUROfusion Consortium, funded by the European Union via the Euratom Research and Training Programme (Grant Agreement No 101052200 — EUROfusion). Views and opinions expressed are however those of the author(s) only and do not necessarily reflect those of the European Union or the European Commission. Neither the European Union nor the European Commission can be held responsible for them.

References

[1] F. Lunardon, et al., The MEST, a new magnetic energy storage and transfer system: application studies to the European DEMO, Fusion Eng. Des. 157 (2020).
[2] E. Gaio, et al., Status and challenges for the concept design development of the EU DEMO plant electrical system, Fusion Eng. Des. 177 (2022), 113052.
[3] J. Tao, et al., ITER coil power supply and distribution system, in: Proceedings of the 2011 IEEE/NPSS 24th Symposium on Fusion Engineering, Chicago, IL, 2011, pp. 1–8.
[4] A. Ferro, F. Lunardon, S. Ciattaglia, E. Gaio, The reactive power demand in DEMO: estimations and study of mitigation via a novel design approach for base converters, Fusion Eng. Des. (2019).
[5] R. Piovan, E. Gaio, F. Lunardon, A. Maistrello, MEST: a new Magnetic Energy Storage and Transfer system for improving the power handling in fusion experiments, Fusion Eng. Des. (2019).